Estimation of Muscle Fiber Conduction Velocity from Surface EMG Recordings by Optimal Spatial Filtering

# Estimation of Motor Unit Conduction Velocity from Surface EMG Recordings by Signal-Based Selection of the Spatial Filters

Luca Mesin[1], Francesca Tizzani[1], Dario Farina[2,*]

*Abstract*— **Muscle fiber conduction velocity (CV) can be estimated by the application of a pair of spatial filters to surface EMG signals and compensation of the spatial filter transfer function with equivalent temporal filters. This method integrates the selection of the spatial filters for signal detection to the estimation of CV. Using this approach, in this study we propose a novel technique for signal-based selection of the spatial filter pair that minimizes the effect of non-propagating signal components (end-of-fiber effects) on CV estimates (*optimal filters*). The technique is applicable to signals with one propagating and one non-propagating component, such as single motor unit action potentials. It is shown that the determination of the optimal filters also allows the identification of the propagating and non-propagating signal components. The new method was applied to simulated and experimental EMG signals. Simulated signals were generated by a cylindrical, layered volume conductor model. Experimental signals were recorded from the abductor pollicis brevis with a linear array of 16 electrodes. In the simulations, the proposed approach provided CV estimates with lower bias due to non-propagating signal components than previously proposed methods based on the entire signal waveform. In the experimental signals, the technique separated propagating and non-propagating signal components with an average reconstruction error of 2.9 ± 0.9% of the signal energy. The technique may find application in single motor unit studies for decreasing the variability and bias of CV estimates due to the presence and different weights of the non-propagating components.**

This work was supported by the European Shared Cost Project Neuromuscular assessment in the Elderly Worker (NEW) (Contract n° QLRT-2000-00139), by the European Shared Cost Project On ASymmetry In Sphincters (OASIS) (Contract n° QLK6-CT-2001-00218), and by the Danish Technical Research Council (project "Centre for Neuroengineering (CEN)", contract n° 26-04-0100).

1. Laboratorio di Ingegneria del Sistema Neuromuscolare (LISiN), Dipartimento di Elettronica, Politecnico di Torino, Torino, Italy

2. Center for Sensory-Motor Interaction (SMI), Department of Health Science and Technology Aalborg University, Aalborg, Denmark

Address for correspondence: * Dario Farina, Ph.D., Center for Sensory-Motor Interaction, Aalborg University, Fredrik Bajers Vej 7 D-3, DK-9220 Aalborg, Denmark, tel: +4596358821; fax: +4598154008, E-mail: df@hst.aau.dk



*Index Terms*— **spatial filtering, conduction velocity, linear electrode arrays**

## I. Introduction

CONDUCTION velocity (CV) reflects membrane muscle fiber properties and is thus indicative of the peripheral condition of the neuromuscular system. It can be estimated from multi-channel surface EMG recordings located between the innervation zone and the tendon region along the direction of the muscle fibers [1][2]. In ideal conditions, the surface action potentials detected along the muscle fibers travel without changes in shape from the innervation zone of the motor unit to the tendon endings, but this condition is never met in practice. Thus, there is not a unique mathematical definition of the delay between detected potentials but many definitions are possible. Each definition corresponds to a delay estimation method [3].

One of the main problems in CV estimation is the presence of non-propagating components associated to the propagating ones. These components are mainly due to the generation and extinction of the action potentials at the innervation and tendon zones [3][4][5]. Different methods for CV estimation have different sensitivities to non-propagating signal components. Moreover, the effect of these components depends on the spatial filter applied for signal detection [6][7]. Specific combinations of spatial filters and estimation methods may be better than others in reducing the bias in CV estimates due to non-propagating signals. Double differentiation of the detected signals [8], for example, provides a non-biased CV estimation in the ideal case in which the non-delayed activity is identical in all channels.

Recently, Farina & Merletti [9] proposed an approach for CV estimation based on the application of a pair of spatial filters and on the estimation of the temporal filters that best align the signals and compensate for the applied spatial filters. The effect of the transfer function of the temporal filters on propagating components is equivalent to that of spatial filters up to a scaling factor on the frequency axis which depends on the delay of propagation. This is due to the relation between temporal and spatial coordinate systems through the velocity of propagation. The estimated delay of propagation is defined as that determining the best matching between the spatially and then temporally filtered signals [9]. This approach combines the selection of the spatial filters for signal detection to the estimation of CV and this allows for the selection of the spatial

filters as those that best attenuate the effect of specific signal components on the delay estimate.

Farina & Merletti [9] indicated how the choice of the spatial filters may influence the estimated CV. Using specific filters they were able to reduce the CV estimation bias due to non-propagating components. However, the selection of the spatial filters was not specifically designed for minimizing the effect of non-propagating signals on the delay estimates.

In this study, we propose a method for the selection of the filter pair which minimizes the effect of non-propagating components on CV estimates starting from the approach proposed in [9]. It will be shown that the derivation of this spatial filter pair allows the estimation of the shapes of the propagating and non-propagating components from the surface EMG. We will limit our analysis to single motor unit recordings, in which, to a first approximation, a single propagating and a single non-propagating waveform are present. The non-propagating part of the single motor unit action potentials is determined by both the generation and the extinction of the action potential, with a predominant contribution of the extinction phenomenon, on which we will focus.

## II. METHODS

### *A. Signal model and notations*

The method is based on the analysis of four surface EMG signals obtained from detection points located along the fiber direction. The model considered is the following:

$$\begin{cases} v_0(t) = v_p(t) + \alpha_0 v_{np}(t) \\ v_1(t) = v_p(t-\tau) + \alpha_1 v_{np}(t) \\ v_2(t) = v_p(t-2\tau) + \alpha_2 v_{np}(t) \\ v_3(t) = v_p(t-3\tau) + \alpha_3 v_{np}(t) \end{cases} \quad (1)$$

where $v_i(t)$ (i = 0,…,3) are the recorded signals, $v_p(t)$ is the propagating signal component, $v_{np}(t)$ the non-propagating component, and $\vec{\alpha} = (\alpha_0, \alpha_1, \alpha_2, \alpha_3)$ the unknown vector of multiplication coefficients applied to the non-propagating signal part. The four signals in model (1) can be either four monopolar derivations or signals obtained by the application of a spatial filter at the four detection points. Model (1) assumes that: 1) the propagating component has the same shape and amplitude in the four recorded channels; 2) the delay between propagating components detected in adjacent channels is constant (i.e., the distance between detection systems is fixed and velocity of propagation is constant along the fiber); and 3) the non-propagating component has the same shape in the four channels and is multiplied by unknown coefficients. If the elements of the vector $\vec{\alpha}$ are all equal, the non-propagating component can be suppressed by any spatial filter with null summation of the weights applied to the four signals. However, in general the entries of the vector $\vec{\alpha}$ are not equal and we will focus on this condition.

In the model described by Eq. (1), the only available data are the recorded signals $v_i(t)$. The delay $\tau$, the shape of the propagating and non-propagating component and its amplitude in the four channels are unknown and should be estimated without any a-priori information. The problem will be solved by defining a specific pair of spatial filters (termed in the following optimal, according to the definition provided below) which allow exact delay estimation. It will be shown that the knowledge of this filter pair allows the determination of all the unknowns in Eqs. (1). Thus, the method will be described in two phases: 1) the derivation of all the elements of model (1) when the optimal filter pair is known, and 2) the determination of the optimal filters pair.

### *B. Estimate of the delay by spatial and temporal filtering*

Given a pair of spatial filters applied to the four detected signals, the delay $\tau$ in model (1) can be estimated from the application of temporal filters that compensate for the spatial filters, as proposed by Farina & Merletti [9]. The method is illustrated in Figure 1. If we first apply two spatial filters and then two temporal filters (with transfer functions of the same shape as the spatial filters and delay set to $\hat{\tau}$) and subtract the resulting signals, the following relation holds (Figure 1):

$$Y_1(f) - Y_2(f) = V_p(f)\left[H_1(f\tau)H_2(f\hat{\tau}) - H_2(f\tau)H_1(f\hat{\tau})\right] + V_{np}(f)\gamma\left(f\hat{\tau}, \vec{\alpha}, \vec{a}, \vec{b}\right) \quad (2)$$

where $V_p(f)$ and $V_{np}(f)$ are the Fourier transforms of the propagating and non-propagating components, respectively, $H_1(f\tau) = \sum_{i=0}^{3}\left(a_i e^{j\pi f\tau(2i-3)}\right)$, $H_2(f\tau) = \sum_{i=0}^{3}\left(b_i e^{j\pi f\tau(2i-3)}\right)$ the transfer functions of the two spatial filters used for detecting the signals, with $a_i$ and $b_i$ (i = 0,…,3) the filter weights. We will assume that the summation of the weights of the two filters is zero. The function $\gamma\left(f\hat{\tau}, \vec{\alpha}, \vec{a}, \vec{b}\right)$ is given by:

$$\gamma\left(f\hat{\tau}, \vec{\alpha}, \vec{a}, \vec{b}\right) = \sum_i \left\{\alpha_i\left[a_i H_2(f\hat{\tau}) - b_i H_1(f\hat{\tau})\right]\right\} = s_1 e^{-3j\pi f\hat{\tau}} + s_2 e^{-j\pi f\hat{\tau}} + s_3 e^{+j\pi f\hat{\tau}} + s_4 e^{+3j\pi f\hat{\tau}} \quad (3)$$

with $s_i = Ab_{i-1} - Ba_{i-1}$, being $A = \vec{\alpha}\cdot\vec{a}$ and $B = \vec{b}\cdot\vec{\alpha}$, and $\hat{\tau}$ the estimated delay defining the scaling of the frequency axis of the temporal filter transfer functions.

The minimization of the energy of the difference signal $Y_1(f) - Y_2(f)$ with respect to the delay $\hat{\tau}$ leads to an estimate $\tau_{est}$ of the delay [9]:

$$\tau_{est} = \arg\min_{\hat{\tau}} e^2$$

$$e^2 = \int |Y_1(f) - Y_2(f)|^2 df = \int \left|V_p\left[H_1(f\tau)H_2(f\tau_{est}) - H_2(f\tau)H_1(f\tau_{est})\right] + V_{np}\gamma\left(f\tau_{est}, \vec{\alpha}, \vec{a}, \vec{b}\right)\right|^2 df \quad (4)$$

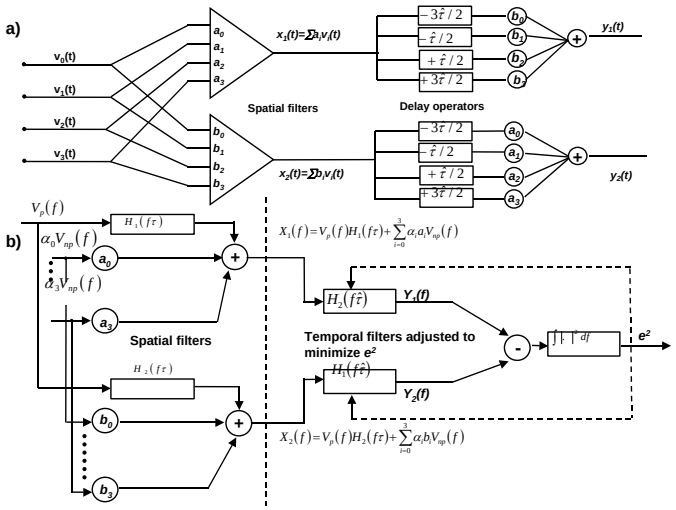


**Figure 1**. Schematic representation of the detection and processing of surface EMG signals for the application of the CV estimator proposed in [Fa03], in both a) time and b) frequency representations. The detection is performed by two spatial filters, which filter the propagating signal Vp(f) with transfer functions which depend on CV (τ is the delay of propagation, directly related to CV). The two filtered signals present components (Vnp with i = 0,…M) which do not propagate along the fiber and which are linearly combined by the weights of the spatial filters. The processing step consists of filtering in the temporal domain the signals previously filtered in the spatial domain and adjusting the transfer functions of the temporal filters in order to obtain two signals most similar to each other. The scheme has been adapted from [9].

As derived in [9], the mean square error in Eq. (4) is the same up to a multiplication factor for filter pairs with the same parameters $\varepsilon, \eta$ defined as:

$$\begin{cases} \varepsilon = a_1 b_0 - a_0 b_1 \\ \eta = a_2 b_0 - a_0 b_2 \end{cases} \quad (5)$$

ε and η define all the filter pairs which lead to different delay estimates, except the pairs resulting from the condition $a_2 b_1 - a_1 b_2 = 0$ [9]. As in [9], we will fix four weights of the filter pair ($a_1 = -1, a_2 = 2; b_1 = 2, b_2 = -1$). This choice allows the inclusion of two double differential filters in the set of spatial filter pairs considered.

Each filter pair provides a different estimation of the delay depending on how the effect of the non-propagating components on the delay estimate is reduced by the spatial filters [thus, depending on $\gamma\left(f\hat{\tau}, \vec{\alpha}, \vec{a}, \vec{b}\right)$]. It is then possible to build an infinite number of delay estimators by changing the spatial filter pair.

*C. Amplitudes of the non-propagating signal components and optimal filters*

In model (1), there is an indeterminacy in the estimation of the amplitude vector $\vec{\alpha} = (\alpha_0, \alpha_1, \alpha_2, \alpha_3)$, since this vector multiplies the non-propagating component $v_{np}(t)$, which is also an unknown of the problem. The vector $\vec{\alpha}$ can be multiplied by any constant value, the signal $v_{np}(t)$ by the inverse of this value, and the observations (recorded signals) in Eqs. (1) will be the same. As a consequence, $\vec{\alpha}$ is estimated up to a multiplicative factor. Without loss of generality, we fix $\alpha_0 = 1$. In addition, we introduce a new parameter K, such that:

$$K = \frac{\alpha_3 - \alpha_1}{1 - \alpha_2} \quad (6)$$

with $\alpha_2 \neq 1$ (the case $\alpha_0 = \alpha_1 = \alpha_2 = \alpha_3 = 1$ is excluded by Eq. (6); as mentioned above, all the filters considered remove the non-propagating components in such a case, so that no filter pair is better than another and optimization is not needed).

Given $\alpha_1$ and $\alpha_2$, $\alpha_3$ is determined by K [Eq. (6)], thus the new unknown parameters are $\alpha_1$, $\alpha_2$, and K. This does not change the number of parameters to be estimated but determines simpler expressions in the following derivations.

Given model (1) and relation (2), a spatial filter pair completely suppresses the non-propagating components in $Y_1$ and $Y_2$ [from Eq. (4)] if it determines $\gamma\left(f\hat{\tau}, \vec{\alpha}, \vec{a}, \vec{b}\right) = 0$, $\forall \hat{\tau}$. We will denote the ε and η coefficients [Eq. (5)] which identify this filter pair as $\varepsilon_{opt}$, $\eta_{opt}$ and we will refer to these two filters as optimal filters. In the following we will show that the knowledge of the optimal filters allows the determination all the terms in Eqs. (1). After this, we will show how to estimate the optimal filters, i.e., $\varepsilon_{opt}$ and $\eta_{opt}$.

$\varepsilon_{opt}$ and $\eta_{opt}$ correspond to the filter pair satisfying the following condition [Eq. (3)]:

$$\gamma\left(f\hat{\tau}, \vec{\alpha}, \varepsilon, \eta, \vec{b}\right) = s_1 e^{-3j\pi f\hat{\tau}} + s_2 e^{-j\pi f\hat{\tau}} + s_3 e^{+j\pi f\hat{\tau}} + s_4 e^{+3j\pi f\hat{\tau}} = 0 \quad (7)$$

Eq. (7) is satisfied for $s_i = 0$ (i = 1,…,4) since the exponential functions are independent of each other. The coefficients $s_i$ depend on $\varepsilon_{opt}$, $\eta_{opt}$ and on the vector $\vec{\alpha}$, since $s_i = Ab_{i-1} - Ba_{i-1} = 0$ (i=1, 2, 3, 4). Eq. (7) defines a system of 4 equations in 5 unknowns: $\varepsilon_{opt}$, $\eta_{opt}$, $\alpha_1$, $\alpha_2$ and *K*. If the rank of the complete matrix of this linear system is maximum (i.e., equal to four), only one degree of freedom remains in the solution. It can be shown that the solution of the system is in this case $\vec{\alpha} = (1, \chi, 1, \chi)$, with $\chi$ arbitrary. This solution is not physically acceptable since it imposes a constraint on the amplitudes of the non-propagating components, which does not hold in general. The other solutions are obtained imposing the rank of the complete matrix of the system to be less than four, which is equivalent to setting [see Eq. (6)]:

$$K = -\frac{\eta_{opt}}{3 + \varepsilon_{opt}}; \ \eta_{opt}(1 - \alpha_2) + (3 + \varepsilon_{opt})(\alpha_3 - \alpha_1) = 0. \quad (8)$$

Eqs. (8) define a relation between the optimal filters and the amplitudes of the non-propagating component. With this condition, the four equations ($s_i = 0$, for i = 1,…,4) derived

from Eq. (7) are linearly dependent (rank equal to 1), and lead to:

$$\alpha_1 = \frac{3\alpha_2 + \varepsilon_{opt} + K(-1+\alpha_2)(3+\varepsilon_{opt})}{3+\varepsilon_{opt}} = c_1\alpha_2 + c_2 \qquad (9)$$

where $c_1 = \frac{3+\eta_{opt}}{3+\varepsilon_{opt}}$, $c_2 = \frac{\varepsilon_{opt}-\eta_{opt}}{3+\varepsilon_{opt}}$. Eq. (9) can be rewritten equivalently as:

$$\varepsilon_{opt}(\alpha_1 - 1) - \eta_{opt}(\alpha_2 - 1) + 3(\alpha_1 - \alpha_2) = 0 . \qquad (10)$$

Eqs. (8), (9), and (10) associate the pair of optimal filters defined by $\varepsilon_{opt}$ and $\eta_{opt}$ to the amplitudes $\alpha_1$, $\alpha_2$ and $\alpha_3$ of the non-propagating component ($\alpha_0 = 1$).

Thus, once the optimal filters are identified, they determine a condition on $\alpha_1$ and $\alpha_2$, and viceversa. This is due to the fact that the knowledge of the optimal filter provides information on the non-propagating component amplitude vector (since the optimal filters are those that compensate for the amplitude vector and cancel out the weight of the non-propagating component). Moreover, given the optimal filters, K is determined by Eqs. (8). Thus, once the optimal filters are determined they allow to obtain the vector $\vec{\alpha}$ up to only one unknown parameter:

$$\vec{\alpha} = (1, c_1\alpha_2 + c_2, \alpha_2, K(1-\alpha_2) + c_1\alpha_2 + c_2) \qquad (11)$$

with $c_1$ and $c_2$ given by Eq. (9). Note that the knowledge of the optimal filters implies $\gamma = 0$ and, in this condition, the minimization of the mean square error in Eq. (4) provides the exact delay $\tau$.

Finally, we note that if $\vec{\alpha}$ is in the form of Eq. (11), the function $\gamma(f\hat{\tau}, \vec{\alpha}, \vec{a}, \vec{b})$ [Eq. (7)] has the same shape for any choice of $\alpha_2$, with only the amplitude depending on $\alpha_2$ (this property can be derived with rather simple algebraic calculations, omitted).

*D. Estimation of the non-propagating component*

Let's suppose to know the optimal filters and, thus, as indicated in the previous section, the shape of $\gamma(f\hat{\tau}, \vec{\alpha}, \vec{a}, \vec{b})$ for any other filter pair, up to an amplitude scaling factor. In this condition, we also have an exact estimate of the delay $\tau$. If the estimated delay $\tau_{est}$ is exact, the first term in Eq. (2) is zero for any choice of the spatial filter pair and an estimate $\hat{V}_{np}$ of $V_{np}$ is thus obtained as:

$$\hat{V}_{np}(f) = \frac{Y_1(f) - Y_2(f)}{\gamma(f\tau_{est}, \vec{\alpha}, \varepsilon, \eta)} \qquad (12)$$

for any spatial filter pair, except for the optimal filters which would lead to $\gamma(f\tau_{est}, \vec{\alpha}, \vec{a}, \vec{b}) = 0$ [Eq. (7)]. Thus, $\gamma(f\tau_{est}, \vec{\alpha}, \vec{a}, \vec{b})$ is obtained from non-optimal filters in Eq. (12), using the delay and the vector $\vec{\alpha}$ derived from the optimal filters. The choice of the filter pair for defining $\gamma(f\tau_{est}, \vec{\alpha}, \vec{a}, \vec{b})$ in Eq. (12) is arbitrary but the larger the energy of $\gamma(f\tau_{est}, \vec{\alpha}, \vec{a}, \vec{b})$ the more robust the estimate of $V_{np}$. Thus, the filter pair should be "far" from the condition of the optimal filters [for which $\gamma(f\tau_{est}, \vec{\alpha}, \vec{a}, \vec{b}) = 0$]. We will refer to this filter pair as worst filters. Such worst filters are defined as those maximizing (for the bounded discrete set of filter pairs considered) the energy of the difference signal $e^2$ defined in Eq. (4) for the correct delay value. Since Eq. (12) is valid for any filter pair (except for the optimal ones), to improve the quality of estimation of the non-propagating component, the expression (12) is applied for all filter pairs corresponding to $e^2$ larger than one fourth of its global maximum (corresponding to the worst filters), and the resulting estimates of $V_{np}$ are averaged. It was verified on simulation (results not shown) that such an averaging reduced the contribution of noise on the estimated non-propagating component.

If the optimal spatial filters are determined, the vector of amplitudes $\vec{\alpha}$ is known except for one parameter [$\alpha_2$ in Eq. (10)]. As stated above, $\alpha_2$ affects only the amplitude of $\gamma(f\tau_{est}, \vec{\alpha}, \varepsilon, \eta)$. Thus, the shape of $V_{np}(f)$ is fully determined from Eq. (12), up to the amplitude.

To reduce the effect of noise on the average, the estimation of the non-propagating component $V_{np}(f)$ (obtained as described above with averaging over a number of filter pairs) is interpolated in time domain with a polynomial function and considered on a bounded temporal support. $N_i$ samples are used for the interpolation on each side of the maximum of $\hat{v}_{np}(t)$. The number of samples to describe the non-propagating component is estimated by considering samples on the left and right side of the maximum of $\hat{v}_{np}(t)$ which satisfy, for each side, the following properties:

1) $\hat{v}_{np}(t_n) < \hat{v}_{np}(t_{n-1})$, where $t_n$ and $t_{n-1}$ are the nth and (n-1)th considered samples;

2) $|\hat{v}_{np}(t_n)| > 0.05|\hat{v}_{np}(t_0)|$, where $t_n$ is the nth considered sample, and $t_0$ corresponds to the maximum of $\hat{v}_{np}(t)$.

The non-propagating component is estimated by polynomial interpolation on the selected samples. The polynomial fit is then truncated at the time interval between the first zeros of the polynomial on the two sides. The degree of the polynomial is chosen as that providing the best approximation of $\hat{v}_{np}(t)$ on this time interval. Since high degree polynomials present large oscillations, the first zeros of the polynomial on the two sides can be estimated badly for too high degrees. For this reason, the degree of the polynomial providing the best fit of the non-propagating component is not always $N_i$.

*E. Estimation of the propagating component*

When the optimal filters are obtained, the vector of amplitudes of the non-propagating components is known up to an unknown term, the non-propagating component is derived

with Eq. (12) (and the subsequent interpolation procedure described above) up to an amplitude factor, and the delay of the propagating component is estimated exactly.

From the non-propagating components we can derive the propagating one. Indeed, under the assumption of known optimal filters, the model described in Eqs. (1) can be written as:

$$\begin{cases} v_0(t) = v_p(t) + B_{amp}\alpha_0\hat{v}_{np}(t) \\ v_1(t) = v_p(t-\tau_{est}) + B_{amp}\alpha_1\hat{v}_{np}(t) \\ v_2(t) = v_p(t-2\tau_{est}) + B_{amp}\alpha_2\hat{v}_{np}(t) \\ v_3(t) = v_p(t-3\tau_{est}) + B_{amp}\alpha_3\hat{v}_{np}(t) \end{cases} \quad (13)$$

where $\hat{v}_{np}(t)$ is the estimated non-propagating term, the amplitude vector $\vec{\alpha}$ is given by Eq. (11), and $B_{amp}$ is the unknown amplitude of the non-propagating term, since $\alpha_0$ has been fixed to 1. The unknowns of system (13) are $\alpha_2$, $B_{amp}$, and $v_p(t)$. Translating and linearly combining the equations in system (13), we obtain:

$$\begin{cases} v_0(t) - v_1(t+\tau_{est}) = B_{amp}\left[\alpha_0\hat{v}_{np}(t) - \alpha_1\hat{v}_{np}(t+\tau_{est})\right] \\ v_1(t) - v_2(t+\tau_{est}) = B_{amp}\left[\alpha_1\hat{v}_{np}(t) - \alpha_2\hat{v}_{np}(t+\tau_{est})\right] \\ v_2(t) - v_3(t+\tau_{est}) = B_{amp}\left[\alpha_2\hat{v}_{np}(t) - \alpha_3\hat{v}_{np}(t+\tau_{est})\right] \end{cases} \quad (14)$$

which is a system of 3 equations in 2 unknowns, with t (the time variable) as a parameter. The system in Eq. (14) can be solved for $B_{amp}$ and $\alpha_2$ selecting any time sample. More robust estimates are obtained by averaging estimates of B and $\alpha_2$ obtained from Eqs. (14) solved through the pseudo-inverse matrix for a number of time samples. For this purpose, the samples for which the estimated non-propagating component is larger than a threshold are used. Outliers due to noise were excluded in the averaging process. An alternative approach for the estimation of $B_{amp}$ and $\alpha_2$, consisting in integrating over time the system (14), provided equivalent results.

Once $B_{amp}$ and $\alpha_2$ are obtained from Eqs. (14), the propagating term is estimated by subtracting the estimated non-propagating term from each of the 4 recorded signals, translated by multiple of $\tau_{est}$ for alignment and averaged:

$$\hat{v}_p(t) = \frac{1}{4}\sum_{k=0}^{3} v_k(t + k\tau_{est}) - \alpha_k B_{amp}\hat{v}_{np}(t + k\tau_{est}) \quad (15)$$

*F. Determination of the optimal filters*

From Eqs. (11)-(15), if the optimal filters are known, all the unknowns in model (1) are determined. Thus, the initial problem of estimating the model parameters in Eq. (1) (including unknown waveforms for the propagating and non-propagating components) is reduced to the estimation of $\varepsilon_{opt}$ and $\eta_{opt}$ which define the optimal filter pair.

It has to be noted that we can apply all the previous equations assuming as optimal any pair of filters, thus obtaining an estimation of the delay, the propagating and non-propagating component. However, only the optimal filters would fit all the hypotheses, i.e., the vanishing of $\gamma\left(f\hat{\tau}, \vec{\alpha}, \vec{a}, \vec{b}\right)$ to compute the vector $\vec{\alpha}$ from Eq. (11) and the assumption that $\tau_{est}$ is an exact estimate of the delay τ. Thus, if we apply the above procedure assuming as optimal a pair of filters which does not satisfy the condition in Eq. (7), the determination of the propagating and non-propagating component will be incorrect. This property can be used to derive the optimal filters. We can select a filter pair and, assuming it corresponds to the optimal filters, we can obtain the propagating and non-propagating components. On the basis of the estimates of the model parameters we can then build the estimated observations (the four recorded signals) and compare them with the actual observations. In case of selection of the optimal filters, the fit will be better than when selecting any other filter pairs. Thus, the optimal filters are those leading to the best reconstruction of the observations. Given the reconstructed observations $\hat{v}_i(t)$, i = 0,…, 3, which depend on the choice of $\varepsilon_{opt}$ and $\eta_{opt}$, the following mean square error is thus minimized over $\varepsilon_{opt}$ and $\eta_{opt}$:

$$err^2 = \frac{1}{4}\sum_{i=0}^{3}\left\|v_i(t) - \hat{v}_i(t)\right\|_2^2 \quad (16)$$

The minimum of the mean square error (16), over $\varepsilon_{opt}$ and $\eta_{opt}$, identifies the two optimal filters. Moreover, the minimum mean square error is indicative of the performance of the method since small mean square errors correspond to good reconstructions and thus to good matching of all the hypotheses of the approach. The method is schematically shown in Figure 2 while Figure 3 reports an example of application on a simulated single fiber action potential. The method is insensitive to the degree of superposition of the two signal components, which can be completely overlapped in the time and frequency domains.

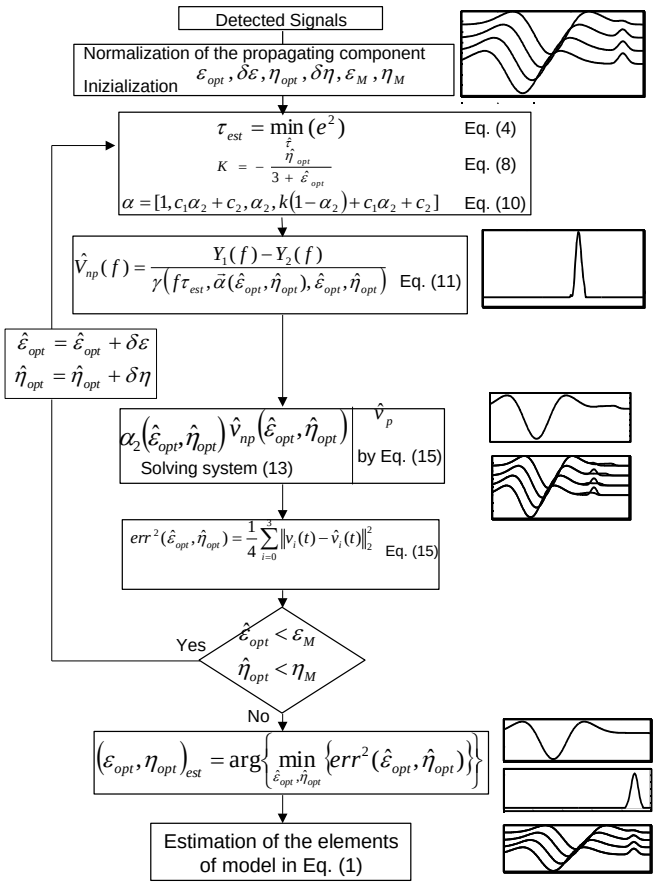


**Figure 2**. Flow-chart of the proposed method. At each step, a pair of candidate optimal filters (corresponding to the family definided by $\hat{\varepsilon}_{opt}, \hat{\eta}_{opt}$) is used to determine the propagating and non-propagating component and to reconstruct the detected signals from these estimates. The pair ($\hat{\varepsilon}_{opt}, \hat{\eta}_{opt}$) resulting in the minimum mean square error in the reconstruction provides the estimation of the delay and of the two signal components. $\hat{\varepsilon}_{opt}$ and $\hat{\eta}_{opt}$ are changed independently. $\varepsilon_m$ and $\eta_m$ indicate the minimum considered values for $\varepsilon$ and $\eta$, $\varepsilon_M$ and $\eta_M$ the maximum values, and $\delta\varepsilon$ and $\delta\eta$ the steps with which they are varied. In the results shown in this study, $\varepsilon_m$ = -3, $\eta_m$ =0, $\varepsilon_M$ =1, $\eta_M$ =4, and $\delta\varepsilon$ = $\delta\eta$ = 0.25.

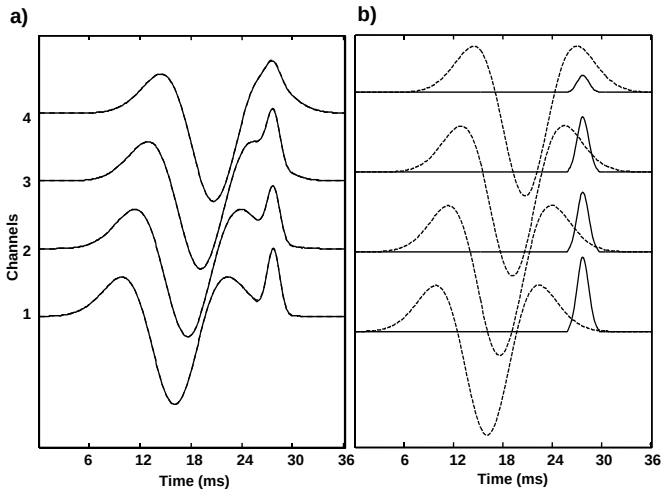


**Figure 3.** Example of application of the proposed method to simulated signals. The propagating component is simulated with the second derivative of a Gaussian function (with standard deviation 14.9 ms) while the non-propagating component is described with a Gaussian function with different amplitude on the four channels (with standard deviation 2.9 ms). a) The simulated signals (solid line) and the reconstructed signals (dashed lines; completely overlapped with the solid lines). b) The estimation of the propagating (dashed lines) and non-propagating components (solid lines).

*G. Simulations*

The proposed method was tested with phenomenological and structure-based surface EMG models. In a first series of simulations, Gaussian signals have been used to test the sensitivity of the method to variations in the shape of the propagating and non-propagating components. In a second simulation set, motor unit action potentials were generated by a cylindrical structure-based model of surface EMG signal which included the bone, muscle, fat, and skin tissues [10]. In these simulations, fat layer thickness was 3 mm, skin layer 1 mm, muscle layer 26 mm, and bone radius 20 mm. Bone, fat, and skin were isotropic (conductivity 0.02 S/m, 0.05 S/m, and 0.5 S/m, respectively), while the muscle tissue was anisotropic with higher conductivity along the fiber direction (longitudinal conductivity $\sigma_l = 0.5$ S/m, transversal conductivity $\sigma_t = 0.1$ S/m). The parameters that varied in the simulations were the fiber depth, fiber length (fibers were symmetric with respect to the end-plate) and signal-to-noise ratio. Using the simulated motor unit action potentials, the proposed method was compared with the spectral matching approach [11] (SM), the method proposed by Farina & Merletti [9] with selection of the spatial filter pair leading to the minimum CV estimate (MCV), and the method of the reference points which computes the delay between peaks in two detected signals after interpolation around the peak with a second order polynomial [12].

*H. Experimental signals*

The proposed method was also applied to experimental surface EMG signals collected from the abductor pollicis brevis muscle of 8 subjects. The signals were detected by a linear array of 16 electrodes (inter-electrode distance 2.5 mm, electrodes 1 mm diameter), located between the most distal tendon and the muscle belly, along the direction of the muscle fibers, and fixed at the skin with adhesive tape. The reference electrode was placed at the wrist. Sixteen monopolar signals were obtained during 60-s long contractions at force lower than 4 % of the maximal voluntary contraction force. The force level was selected during a preliminary phase and corresponded to a level which allowed the identification of single motor unit activities from the surface EMG recordings [13]. Monopolar surface EMG signals were amplified (EMG amplifier, EMG-16, LISiN-OT Bioelectronica, Torino, Italy, bandwidth 10-500 Hz), sampled at 2048 Hz, and stored after a 12 bit A/D conversion. Common mode components due to line interference were minimized by using a negative feedback loop conceptually equivalent to the driven-right-leg circuit [14].

From the monopolar signals, bipolar derivations were obtained off-line and decomposed to identify single motor unit action potentials with a recently proposed decomposition method [15]. The detected times of occurrences of single motor units were used for spike-triggered averaging the monopolar signals in order to obtain the monopolar potentials as recorded at the 16 electrodes of the array [16]. These potentials included propagating and non-propagating components. The four channels in the middle between the innervation zone and tendon were used for further analysis. Before applying the proposed method, the experimental signals were normalized with respect to the minimum value in order to compensate for possible variations in the amplitude of the propagating component across the channels. The reconstruction error was considered as an index of performance in the separation of the propagating and non-propagating component, as discussed above.

## III. Results

### *A. Stability of the method*

The effect of perturbations in the delay and in the width and amplitude of the propagating and non-propagating components on the performance of the method was tested on simulated signals (as described in section G above). For this purpose, the propagating signal was described by the second derivative of a Gaussian function:

$$v_p(t) = \frac{d^2}{dt^2} e^{-\frac{(t-\mu_p)^2}{2\sigma_p^2}} \tag{17}$$

The non-propagating component was modeled as a Gaussian function:

$$v_{np}(t) = e^{-\frac{(t-\mu_{np})^2}{2\sigma_{np}^2}} \tag{18}$$

*A.1 Perturbation of the width and amplitude of the propagating component*

Width and amplitude changes in the propagating component were obtained by changing the variance $\sigma_p$ in Eq. (17):

$$\sigma_p^p = \frac{100+p}{100}\sigma_p \tag{19}$$

where $\sigma_p^p$ is the perturbed width index of the propagating component.

Figure 4a reports an example of determination of the two signal components in case of perturbations of the amplitude and width. Figure 4d shows the CV estimates for width changes in the third channel with p in the range 0-20 [Eq. (19)].

*A.2 Perturbation of the width and amplitude of the non-propagating component*

Perturbation of the width and amplitude of the non-propagating component was obtained by varying the width of the Gaussian function in Eq. (18):

$$\sigma^p{}_{np} = \frac{100+p}{100}\sigma_{np} \tag{20}$$

where $\sigma^p{}_{np}$ is the perturbed width.

An example of reconstruction is shown in Figure 4b. Figure 4e reports the CV estimates for the cases of width changes in the second channel between 0% and 100%.

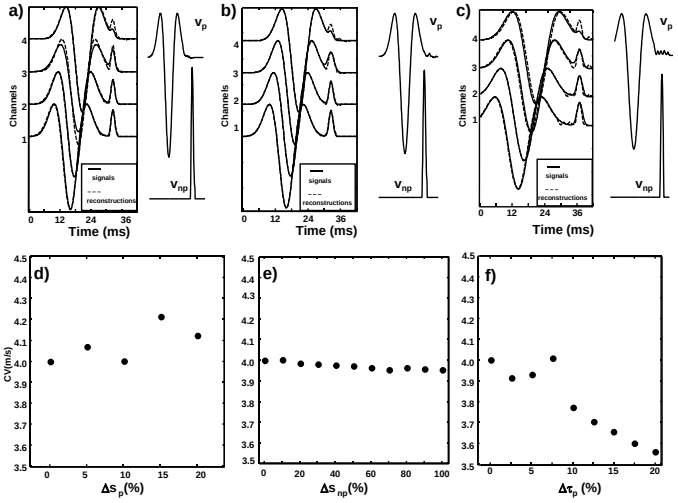


**Figure 4.** Examples of reconstructed (dashed lines) signals and CV estimates when some of the hypotheses of model (1) are not met (signals are modeled as in Figure 3). The width and amplitude of the propagating component are not the same for the different channels in a) and d); the shape of the non-propagating component is not the same for the different channels in b) and e); the delay between adjacent channels is not constant in c) and f). In a) $\sigma_{np} = 6 \cdot \Delta t$, $\sigma_p = 30 \cdot \Delta t$ ($\Delta t$ being the time step, the inverse of the sampling frequency $f_s = 2048$Hz) for the first, second, and fourth channel, $\sigma^p{}_p = 1.15 \cdot \sigma_p$ for the third channel. In d) the width

changes in the third channel between *p*=0 and *p*=20 [*p* given in Eq. (18)]. In b) $\sigma_{np} = 6 \cdot \Delta t$, $\sigma_p = 30 \cdot \Delta t$ for the first, second, and fourth channel, $\sigma^p{}_{np} = 1.7 \cdot \sigma_{nt}$ for the third channel. In e) the CV estimates are reported for the cases of width changes for the non-propagating component in the second channel between 0% and 100%. In c) a perturbation of the delay is introduced in the second channel and an example of reconstruction is shown for the case $p = 15$. In f) the CV estimates are reported for the cases of percentage of variation of $\tau_p$ between 0% and 20% of the value of $\tau$.

*A.3 Perturbation of the delay*

Perturbations of the delay were assessed imposing for the third channel a delay of the propagating component slightly different than $\tau$:

$$\tau_p = \frac{100+p}{100}\tau \quad . \tag{21}$$

An example of reconstruction is shown in Figure 4c for the case $p = 15$. Figure 4f shows the CV estimates with percent increases of $\tau_p$ in the range 0% - 20%.

*B. Simulations of motor unit action potentials*

Figure 5 reports the comparison of the proposed method for CV estimation with SM and MCV for simulated motor unit action potentials. Figure 5a shows the separation of propagating and non-propagating components for a simulated signal generated by a motor unit with 50 fibers, at 7 mm depth within the muscle, with semi-fiber length 50 mm, and signal-to-noise ratio 15 dB. The scatter of end-plates and tendon regions was 5 mm. The CV estimates with the new method, the SM [11] and MCV [9] methods are shown in Figure 5b,c,d for various fiber depths, semi-lengths, and signal-to-noise ratios. It is noted that the method proposed led to the minimum bias of CV estimates among the three methods tested. The method of the reference points applied to the two double differential derivations of the simulated signals poorly performed for increasing fiber depth since the signal energy was mostly due to the non-propagating component and thus the signal-to-noise ratio for the propagating component (used for the computation of the peak delay) was very low. Thus, additional simulations were performed to compare the new method proposed and that of the reference point for varying signal-to-noise ratio. For a motor unit at 4 mm depth into the muscle and 50 mm fiber semi-length the estimates of conduction velocity for the new method and the method of the reference point, respectively, were 4.04 ± 0.13 m/s and 3.89 ± 0.22 m/s (20 dB), 4.02 ± 0.24 m/s and 4.04 ± 0.60 m/s (16 dB), 4.19 ± 0.40 m/s and 4.48 ± 0.86 m/s (12 dB), 3.80 ± 0.37 m/s and 4.30 ± 1.01 m/s (8 dB). Thus, the method of the reference points showed a larger standard deviation and bias of estimation when compared with the proposed method, especially for low signal-to-noise ratios. This is due to the limited amount of information on the waveform used by the method of the reference points. Similarly, local perturbations of the signal shape which affect the peak of the signal have a larger effect on the estimates based on signal peaks than on estimator which use the entire waveform.

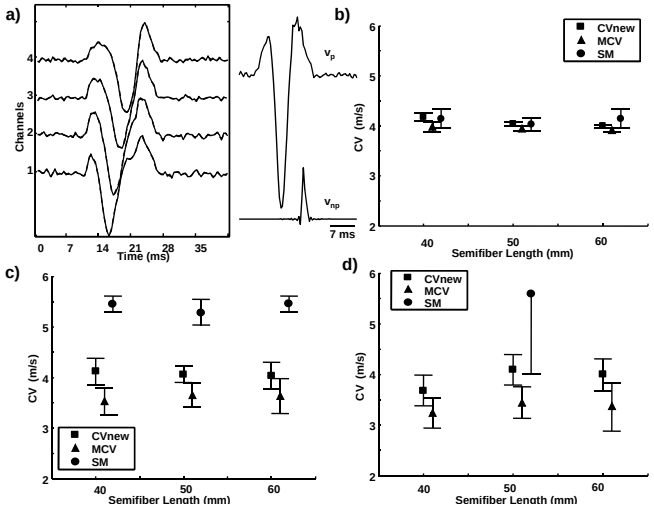


**Figure 5.** Comparison between the proposed method ($CV_{new}$), spectral matching [11] (SP) and minimum CV estimate [9] (MCV) for simulated monopolar motor unit action potentials, using the model described in [10] (skin layer thickness 1 mm, conductivity $\sigma = 0.5 \quad S/m$, fat layer thickness 3 mm, conductivity $\sigma = 0.05 \quad S/m$, muscle thickness 26 mm, longitudinal conductivity $\sigma_l = 0.5 \quad S/m$, transversal conductivity $\sigma_t = 0.1 \quad S/m$, bone radius 20 mm, conductivity $\sigma = 0.02 \quad S/m$). In all cases, the motor unit had 50 fibers randomly distributed in a circular territory (motor unit fiber density 20 fibers/mm$^2$). The scatter of the end-plates and tendon endings was 5 mm in all cases. The inter-channel distance was 5 mm. (a) Example of reconstruction (dashed line) of a motor unit action potential (four monopolar recordings) with depth of the center of the motor unit territory within the muscle 7 mm, semi-fiber length 50 mm, signal-to-noise ratio 15 dB (left plots). The reconstructed signals is almost identical to the original one, thus the two signals are completely superimposed. The propagating and non-propagating parts of the signal, as extracted by the method, are also shown (right plot). CV estimates (mean ± SD, over 20 noise realizations in each condition) from signals generated by motor units with mean semi-fiber length in the range 40-60 mm, and depth 1 mm (b), 4 mm (c) and 7 mm (d) within the muscle. Signal-to-noise ratio 15 dB in all cases. Symbols not shown are out of the reported range of CV values.

*C. Experimental signals*

From the set of identified motor units, we excluded from the analysis those resulting in CV estimates larger than 7 m/s. This

occurred for four out of 13 identified motor units. The method was thus applied to a total of nine motor units from the eight investigated subjects. Figure 6 reports an example of separation of propagating and non-propagating components for one of these motor units. The average (±SD) reconstruction error over the 9 experimental motor unit action potentials was 2.9 ± 0.9 % of the signal energy, indicating good identification of the two signal components.

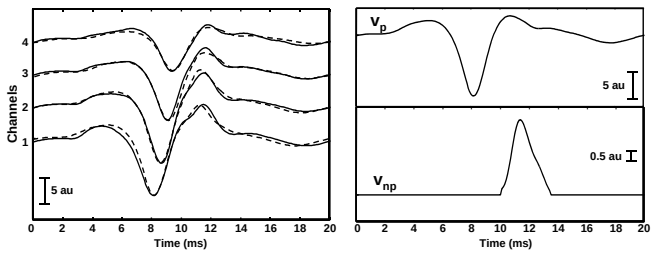


**Figure 6.** Example of application of the proposed method to the separation of propagating and non-propagating components from an experimental monopolar single motor unit recording. (a) The reconstructed signals are shown in dashed lines while the original recordings are in solid lines. (b) The two separated components. The reconstructed propagating component is normalized with respect to the minimum value of the original signal for comparison.

## IV. Discussion

A method for the identification of propagating and non-propagating signal components based on optimal spatial filter pairs was proposed. The starting point for this method is the approach for CV estimation proposed by Farina & Merletti [9], which integrates the selection of spatial filters for EMG signal detection with the method for CV estimation. According to this technique, surface EMG signals are first spatially and then temporally filtered. The spatial and temporal filters are equivalent for propagating components up to a scaling factor on the frequency axis, which reflects the relation between time and space for propagating waves. Two signals filtered by different spatial filters are identical after the application of two temporal filters which compensate for the transfer functions of the spatial filters.

This study focused on the application of this approach for the identification of the propagating and non-propagating components in single motor unit signals detected by linear electrode arrays. This allowed an estimation of CV in principle not affected by end-of-fiber components [see Eq. (4) for $\gamma = 0$]. The method is based on the relation between the coefficients of the spatial filters that remove the non-propagating components and the amplitude of non-propagating signals at the different electrodes. Since the spatial filters produce a linear combination of the non-propagating components, the knowledge of the weights of the filters which cancel out these components provide information on their amplitude and thus allows the reconstruction of the shape of the propagating and non-propagating signal parts. It has thus been shown that knowledge of the spatial filters that show this cancellation property allows the determination of all the unknown elements of the model of signal generation.

A few previous methods have been proposed for separating propagating and non-propagating components from surface EMG signals. Rubio et al. [17][18] used a neural network for this purpose, assuming non-propagating signals with different amplitudes and equal shape on the detected channels. His method was, however, very sensitive to additive noise [17][18] and could not be applied in practical cases. The method proposed in this study is based on an innovative approach and provides lower CV estimation bias with respect to previous techniques (Figure 5). Moreover, its sensitivity to noise is comparable to previous approaches which make use of the entire signal waveform (Figure 5). It has to be noted that in ideal conditions of absence of noise and of shape variations in the signals, correct estimates of delay may be obtained by considering only part of the waveforms, for example the peak [12]. However, local methods are more sensitive to noise, as shown in this study, than the one proposed. In cases in which averaging processes can be performed, noise and shape variations may not be a problem and thus the use of reference points for delay estimation may be the less sensitive to non-propagating signals. However, in studies dealing with single action potential CV the signal-to-noise ratio is usually poor [3] and methods more robust to noise are necessary. The relations between spatial filter pairs and non-propagating components are also important from the theoretical point of view since they add to the spatial filter theory. Important limitations of this approach should, however, be considered.

The method can only be applied to single motor unit recordings and not to the interference surface EMG signal. Indeed, the derivations of the method are based on a model with a single non-propagating and a single propagating component [Eqs. (1)]. The detection of single motor unit action potentials requires a pre-processing of the signal, either based on surface EMG signal decomposition [15][16] or on spike-triggered averaging of the surface EMG after intramuscular EMG decomposition [19].

The analytical method used to derive the method is rather simple [Eq. (1)]. In particular, the model assumes that the non-propagating component has the same shape on all channels, which does not occur exactly in practical cases. The relations between the optimal spatial filters and the amplitude of the non-propagating components, and thus the estimation of the shapes of the two components, are based on this hypothesis. In practical cases, the hypothesis can be reasonably well satisfied depending on the recording conditions. The sensitivity analysis provided in this study by simulation indicates the limitations of the approach when some of the hypotheses of the model in Eqs. (1) are not met (Figure 4). These problems were probably the reason for the failure of the method when applied to experimental motor unit recordings in four out of 13 motor units. However, simulations with the structure-based model have shown that the method performs better than previously available ones on realistic simulated action potentials which do not exactly match all the hypothesis of the method.

In conclusion, we proposed a novel approach for selecting pairs of spatial filters that remove the influence of non-

propagating signal components on the estimation of CV. The determination of this filter pair also allows the separation and estimation of the propagating and non-propagating components from the EMG recordings. The technique provides additional results on spatial filter theory and may find application in single motor unit studies for decreasing the bias and variance of CV estimates due to different weights of the non-propagating components in different recordings, muscles and/or subjects.

## REFERENCES

[1] L. Arendt-Nielsen and M. Zwarts, "Measurement of muscle fiber conduction velocity in humans: techniques and applications", *J. Clin. Neurophysiol*., vol. 6, pp. 173-90, 1989.
[2] D. Farina, W. Muhammad, E. Fortunato, O. Meste, R. Merletti and H. Rix, "Estimation of single motor unit conduction velocity from surface electromyogram signals detected with linear electrode arrays", *Med. Biol. Eng. Comput*., vol. 39, pp. 225-36, 2001
[3] D. Farina, R. Merletti, "Methods for estimating muscle fiber conduction velocity from surface electromyographic signals", *Med. Biol. Eng. Comput*., vol. 42, pp. 432-445, 2004.
[4] N.A. Dimitrova, G.V. Dimitrov and Z.C. Lateva., "Influence of the fiber length on the power spectra of single muscle fiber extracellula rpotentials", *Electromyogr. Clin. Neurophysiol*., vol. 31, pp. 387-98, 1991.
[5] D. Farina, C. Cescon, R. Merletti, "Influence of anatomical, physical, and detection-system parameters on surface EMG", *Biol Cybern*., vol. 86, pp. 445-56, 2002.
[6] E. Schulte, D. Farina, G. Rau, R. Merletti and C. Disselhorst-Klug, "Single motor unit analysis from spatially filtered surface electromyogram signals. Part 2: Conduction velocity estimation", *Med. Biol. Eng. Comput*., vol. 41, pp. 338-45, 2003.
[7] D. Farina, L. Mesin, S. Martina, R. Merletti, "Comparison of spatial filter selectivity in surface myoelectric signal detection: influence of the volume conductor model", *Med. Biol. Eng. Comput*., vol. 42, pp. 114-20, 2004.
[8] H. Broman, G. Bilotto, C. De Luca, "A note on non invasive estimation of muscle fiber conduction velocity", *IEEE Trans. Biomed. Eng*., vol. 32, pp. 341-343, 1982.
[9] D. Farina, R. Merletti., "A novel approach for estimating muscle fiber conduction velocity by spatial and temporal filtering of surface EMG signals", *IEEE Trans. Biomed. Eng*., vol. 50, pp. 1340-51, 2003.
[10] D. Farina, L. Mesin, S. Martina, "A Surface EMG generation model with multylayer cylindrical description of the volume conductor", *IEEE Trans. Biomed. Eng*., vol. 51, pp. 415-26, 2004.
[11] K.C. McGill, L.J. Dorfman, "High-resolution alignment of sampled waveforms", *IEEE Trans. Biomed. Eng*., vol. 31, pp. 462-8, 1984.
[12] T.I. Arabadzhiev, G.V. Dimitrov, N.A. Dimitrova, "Simulation analysis of the ability to estimate motor unit propagation velocity non-invasively by different two-channel methods and types of multi-electrodes", *J. Electromyogr. Kinesiol*., vol. 13, pp. 403-15, 2003.
[13] D. Farina, M. Gazzoni, F. Camelia, "Low-threshold motor unit membrane properties vary with contraction intensity during sustained activation with surface EMG visual feedback", *J. Appl. Physiol.*, vol. 96, pp. 1505-15, 2004.
[14] B. Winter, J. Webster, "Driven-right-leg circuit design," IEEE Trans. Biomed. Eng., vol. 30, pp. 62–66, 1983.
[15] M. Gazzoni, D. Farina, R. Merletti, "A new method for the extraction and classification of single motor unit action potentials from surface EMG signals", *J. Neurosci. Methods*, vol. 136, pp.165-77, 2004
[16] C. Disselhorst-Klug, G. Rau, A. Schmeer, J. Silny, "Non-invasive detection of the single motor unit action potential by averaging the spatial potential distribution triggered on a spatially filtered motor unit action potential", *J. Electromyogr. Kinesiol*., vol. 9, pp. 67-72, 1999.
[17] J. Rubio, R. Merletti, Y. Fan, "Separation of travelling from non-travelling components in surface myoelectric signals", *Proc. VI Mediterranean Conference on Medical and Biological Engineering*, vol. I, July 5-10, 1992, Capri, Italy.
[18] R. Vela, "Characterization and separation of propagating and stationary myoeletric signals", *Master Thesis*, Boston University, 1990
[19] D. Farina, L. Arendt-Nielsen, R. Merletti, T. Graven-Nielsen, "Assessment of single motor unit conduction velocity during sustained contractions of the tibialis anterior muscle with advanced spike triggered averaging", *J. Neurosci. Methods*, vol. 115, pp. 1-12, 2002.

Luca Mesin graduated in electronics engineering in December 1999 from Politecnico di Torino, Torino, Italy, he received the Ph.D. in Applied Mathematics in 2003, from the same university. Since March 2003, he is a Fellow of the Laboratory for Neuromuscular System Engineering in Torino. He was involved in research activities in the fields of Kinetic theory and Deformable Porous Media theory, with applications to Biomathematics and Composite Materials. Now, his main research interests concern signal processing of biomedical signals and modeling of biological systems.